Frequency Locked Loop in Estimating Active, Reactive, and Apparent Powers

Meris Lihić[1], Slobodan Lubura[2]
[1]International Burch University, Sarajevo, Bosnia and Herzegovina
[2]University of East Sarajevo, East Sarajevo, Bosnia and Herzegovina
meris.lihic@stu.ibu.edu.ba
slobodan.lubura@ibu.edu.ba

Original research

Abstract: *In this paper, a new power calculation method has been presented. This method is based on a second-order generalized integrator frequency locked loop (SOGI-FLL) and has enhanced features over classical methods for power calculation widely used in industry. The FLLs have a wide variety of applications such as power converters, grid synchronization, sensorless flux estimation, and control of motor drives. The nature of the FLL allows for it to be a potentially perfect calculation method for power calculation. The obtained results showcase the effectiveness of the proposed power calculation method.*

Keywords: Power measurement, addition theorems for trigonometry, DC component elimination, gain normalization, grid frequency synchronization, MAF filters, MATLAB/Simulink.

1. Introduction

Renewable energies have become important due to the classic electricity infrastructure turning towards a distributed power generation system [1]. Thus, the role of an interface between generation systems and the electricity network will be filled in by the electricity networks of the future, which will extensively use power electronic devise, information and communication technology applications [2]. The power converters, grid-connected, must be carefully designed and controlled to achieve an optimal and efficient operation in distributed power generation systems [3].

One important issue in this distributed power generation system is power measurement in each internal connecting point of the power system. Typically, power calculation methods inherently have built-in zero-crossing detection (ZCD) of grid voltage and current. But, ZCD suffers from voltage (current) sags, drops, spikes and it is not a reliable scheme. As consequence, the power calculation method fails.

In this paper, a new power calculation method has been presented. This method is based on Frequency Locked Loop (FLL) and has enhanced features over classical methods (ZCD) for power calculation widely used in industry. The FLL is a non-linear closed-loop system that can be used in a wide variety of applications such as grid synchronization, flux estimation, and control of motor drives without using sensors [4].

2. Methodology

The first stage of this paper was based on state of art. Due to the nature of the paper, proper research had to be performed, as the FLLs are a rather unexplored topic. Such issues are the complexity of the proposed algorithms, DC offset which makes approximations impossible, the sensitivity of integral-based calculations to external sources, which are the focus of this paper.

The second stage was to develop a mathematical model for the issued problem. The power calculation algorithm is based on addition theorems for trigonometry. By separating the voltage and current into respective *v's* and I've components by using the FLL, and applying addition theorems to them, a simple way to calculate active and reactive power is achieved.

The third stage was to perform simulations using the Matlab/Simulink software. Simulation results confirmed the effectiveness for both the power measuring algorithm, as well as FLL in the task of estimating rapid frequency change.

The fourth stage is to prepare the system for implementation onto an FPGA board. This step has yet to be performed, due to its nature and size, and is intended to be performed in future work.

3. Proposed Power Calculation Method Based on SOGI-FLL

SOGI-FLL Short Overview

The generalized integrator (GI) is the basis in the implementation of most FLLs. Roughly speaking, the GI's structure is based on a double integrator which provides an infinite gain at its resonant frequency and behaves as the amplitude integrator of sinusoidal signals. There are various realizations of the GI. The most popular way of implementing the FLL-based synchronization techniques, which is the focus of this paper, is the second-order generalized integrator (SOGI) [5].

The SOGI-FLL is a simple, and yet valuable tool because, in addition to providing filtered in-phase and quadrature-phase versions of its input, it can directly estimate frequency, and indirectly the phase angle and amplitude of the signal. The SOGI-FLL, nevertheless, has a limited filtering capability. In other words, in the presence of DC offset, harmonics, and inter-harmonics,

the estimated quantities by the SOGI-FLL suffer from ripples [5].

The SOGI-FLL estimates the frequency of the input signal. The frequency of the input signal does not experience sudden changes. Consequently, the FLL algorithm shows greater performance, when the phase angle of the input signal changes, than its PLL-based counterpart [1]. This GI is based on the principle that the time-domain convolution product of a sinusoidal function, by itself, gives rise to the original function which is multiplied by the time variable. Therefore, a processing block with a transfer function that is equal to the Laplace transform of a sinusoidal function (i.e., a resonator), will behave as an "amplitude integrator" for a sinusoidal signal applied at the input. Additionally, the in-quadrature combination of the sine and cosine transfer functions leads to an "ideal integrator" which is independent of the phase angle of the sinusoidal input signal [1].

Proportional-resonant controllers are based on the GI. Also, the GI has been applied to adaptive filtering applications and the PLL implement structure of this filter is shown in Fig. 1, where it is seen that the resonance frequency of the second-order generalized integrator (OGI) is an external parameter called ω'.

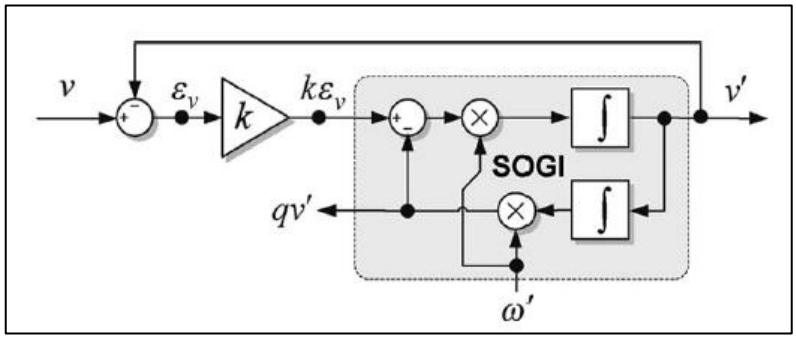

FIGURE 1. Block diagram of OGI [1].
The transfer function of the SOGI is given by:

$$\text{SOGI}(s) = \frac{v}{k\varepsilon_v}; (s) = \frac{\omega s}{s^2\omega'^2} \tag{1}$$

The resonance frequency is noted as ω', in general case, so it differs from the input frequency ω.

The two in-quadrature output signals of the adaptive filer in Fig. 1, i.e., v' and qv', are defined by the following transfer functions:

$$D(s) = \frac{v'}{v}(s) = \frac{k\omega' s}{s^2 + k\omega' s + \omega'^2} \tag{2a}$$

$$Q(s) = \frac{qv'}{v} = \frac{k\omega'^2}{s^2 + k\omega' s + \omega'^2} \tag{2b}$$

As (2a) shows, the bandwidth of the bandpass filter is determined by the gain k and is independent of the central frequency ω'. The same happens with the low-pass filter of (2b), in which the static gain only depends on gain k [1].

The figure below represents an exemplary SOGI-FLL synchronization system. The input grid frequency ω is directly detected by the FLL. On the other hand, the phase angle and amplitude of the input ought to be calculated indirectly.

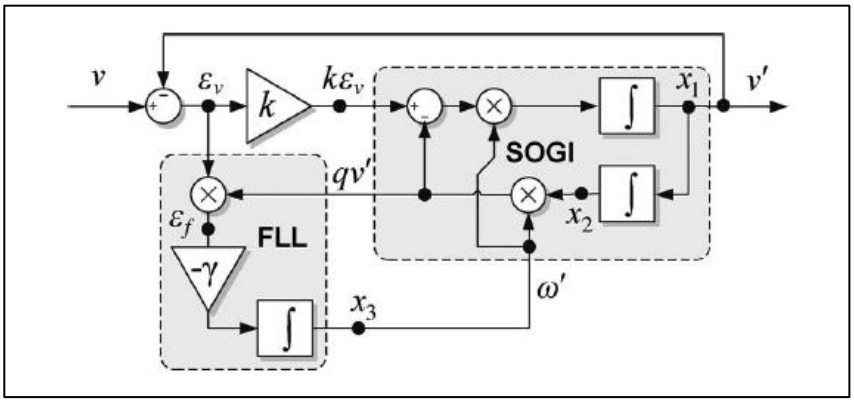

FIGURE 2. SOGI-FLL, a single-phase grid synchronization system [1].

The transfer function from the input signal v to the error ε_v is given by:

$$E(s) = \frac{\varepsilon_v}{v}(s) = \frac{s^2 + \omega'^2}{s^2 + k\omega' s + \omega'^2} \tag{3}$$

A frequency error ε_f is defined as the product of qv' by ε_v. The average value of the error ε_f will be positive when $\omega < \omega$', zero when $\omega = \omega$', and negative when $\omega > \omega$', where are ω' - resonance frequency (eg. 50 Hz) and ω – input grid frequency. As shown in Fig. 2, the DC component of the estimated frequency error can be made zero by shifting the SOGI resonance frequency ω' until it matches the grid frequency on the input ω. This is achieved by an integrated controller with a negative gain $-\gamma$.

In this case, the linear control analysis techniques cannot be applied directly to set the value of the FLL gain γ due to the frequency adaptation loop being nonlinear. As seen in [6], the averaged dynamics of the FLL with $\omega' \approx \omega$ can be described by:

$$\dot{\bar{\omega}}' = -\frac{\gamma V^2}{k\omega'}(\bar{\omega}' - \omega) \tag{4}$$

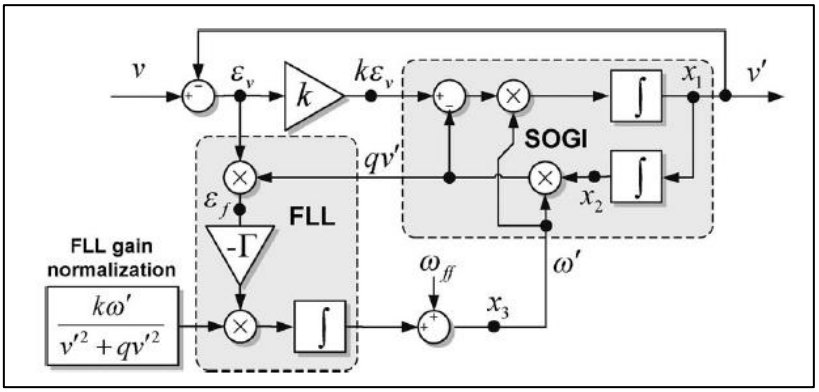

FIGURE 3. SOGI-FLL with feedback-based FLL gain normalization [1].

According to the equation (4) the value of γ can be normalized:

$$\gamma = -\frac{k\omega'}{V^2}\Gamma \tag{5}$$

to obtain the feedback-based linearized system shown in Fig. 4. This system does not depend on either the grid variables or the SOGI-QSG gain.
The FLL gain normalization block, shown in Fig. 3, computes the SOGI control parameter k as well as the output variables ω' and $V^2 = v'^2_2 + qv'^2$ to achieve the response linearization of the FLL. The time constant Γ is the parameter for setting the dynamics of the frequency estimation.

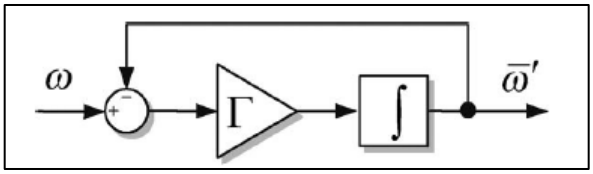

FIGURE 4. Simplified frequency adaptation system of the FLL [1].

The transfer function of the first-order frequency adaptation loop in Figure 4 is given by:

$$\frac{\overline{\omega}'}{\omega} = \frac{\Gamma}{s+\Gamma} \tag{6}$$

The settling time is highly dependent on the gain parameter Γ and can be approximated by:

$$t_{s(FLL)} \approx \frac{5}{\Gamma} \tag{7}$$

FIGURE shows the time response of SOGI-FLL with k = 2 and Γ = 50 when the frequency of the input grid signal suddenly varies from 50 to 45 Hz. As the figure shows, the detected frequency fits a first-order exponential response. The settling time is 100 ms, which matches with the calculation in equation (7) [1].

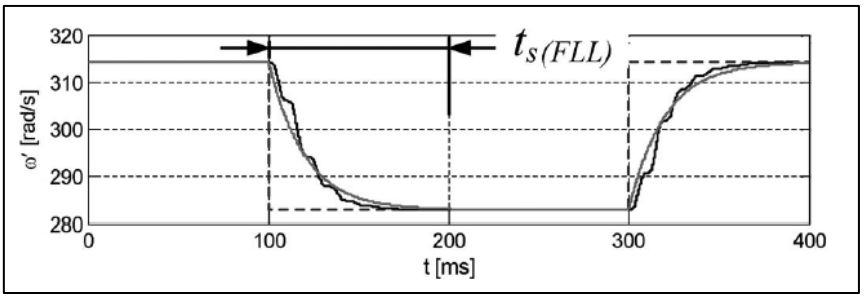

FIGURE 5. Time response of FLL in presence of a frequency step [1].

One important thing to conclude, regarding the frequency estimation, is that the FLL system estimates the frequency error, $\Delta\varepsilon_f$. Let us suppose step change frequency $\Delta\varepsilon_f$ at the input of the FLL. Laplace transformation of the step change frequency is given with $\frac{\Delta\varepsilon f}{s}$. Using the final value theorem (8), it is easy to prove that in the steady-state, FLL estimates step frequency change $\Delta\varepsilon_f$ (9).

$$\lim_{t\to\infty} f(t) = \lim_{s\to 0} sF(s) \tag{8}$$

$$\lim_{s\to 0}\left(s * \frac{\Gamma}{s+\Gamma}(s) * \frac{\Delta\varepsilon_f}{s}\right) = \Delta\varepsilon_r \tag{9}$$

By plugging s to be zero, the expression goes to $\Delta\varepsilon_f$, proving and simplifying the conclusion regarding the frequency estimation.

Proposed power calculation method

Power calculation, for the measurement system proposed in this paper, is performed using addition theorems from trigonometry. Since the SOGI-FLL subsystem gives two output components of voltage/current in quadrature (phase-shifted for $\pi/2$), *v'* and *qv'* or *i'* and *qi'* (Figure 2) respectively, they can be used to calculate powers rather simplistically. Considering that values *v'*, *qv'*, *i'* and *qi'* are $Vcos\varphi_u$, $Vsin\varphi_u$, $Icos\varphi_i$ and $Isin\varphi_i$, these fit perfectly into trigonometric addition theorems.

$$Vsin\varphi_u * Isin\varphi_i + Vcos\varphi_u * Icos\varphi_i = VI(cos\varphi_u cos\varphi_i + sin\varphi_u sin\varphi_i) \tag{10}$$

From equation (10), the right side represents the cosine addition theorem cos(α-β). By applying the mentioned theorem, the following is true.

$$P = Vmax * Imax(cos\varphi)/2 \tag{11}$$

Since most power measurement systems consider RMS values, equation (11) can be rewritten in form:

$$P = \frac{V_{max}the}{\sqrt{2}} * \frac{I_{max}}{\sqrt{2}}(cos\varphi) \tag{12}$$

or:

$$P = V_{rmsilarly} * I_{rms}(cos\varphi) \tag{13}$$

Sim , reactive power can be calculated.

$$Q = V_{rms} * I_{rms}(sin\varphi) \tag{14}$$

Equation (14) is obtained from the sine addition theorem, which is simply achieved by:

$$Vsin\varphi_u * Isin\varphi_i - Vcos\varphi_u * Icos\varphi_i = VI(cos\varphi_u sin\varphi_i - sin\varphi_u cos\varphi_i) \tag{15}$$

According to equations (13) and (14), apparent power (S) can be calculated as follows:

$$S = \sqrt{P^2 + Q^2} = \sqrt{\left(V_{rms} * I_{rms}(cos\varphi)\right)^2 + \left(V_{rms} * I_{rms}(sin\varphi)\right)^2} \tag{16}$$

When solved:

$$S = V_{rms} * I_{rms} \tag{17}$$

From equations (13) and (17), power factor ($cos\varphi$) can be calculated as follows:

$$cos\varphi = \frac{P}{S} \tag{18}$$

With equation (18), all parameters for power calculation are complete.

4. Results and discussion

Performance of the suggested power measuring algorithm, for calculating the active (P), reactive (Q) and apparent (S) powers, were tested in Matlab/Simulink. The model of the suggested algorithm is shown in the following picture.

FIGURE 6 (on the next page). FLL Power Measuring System.

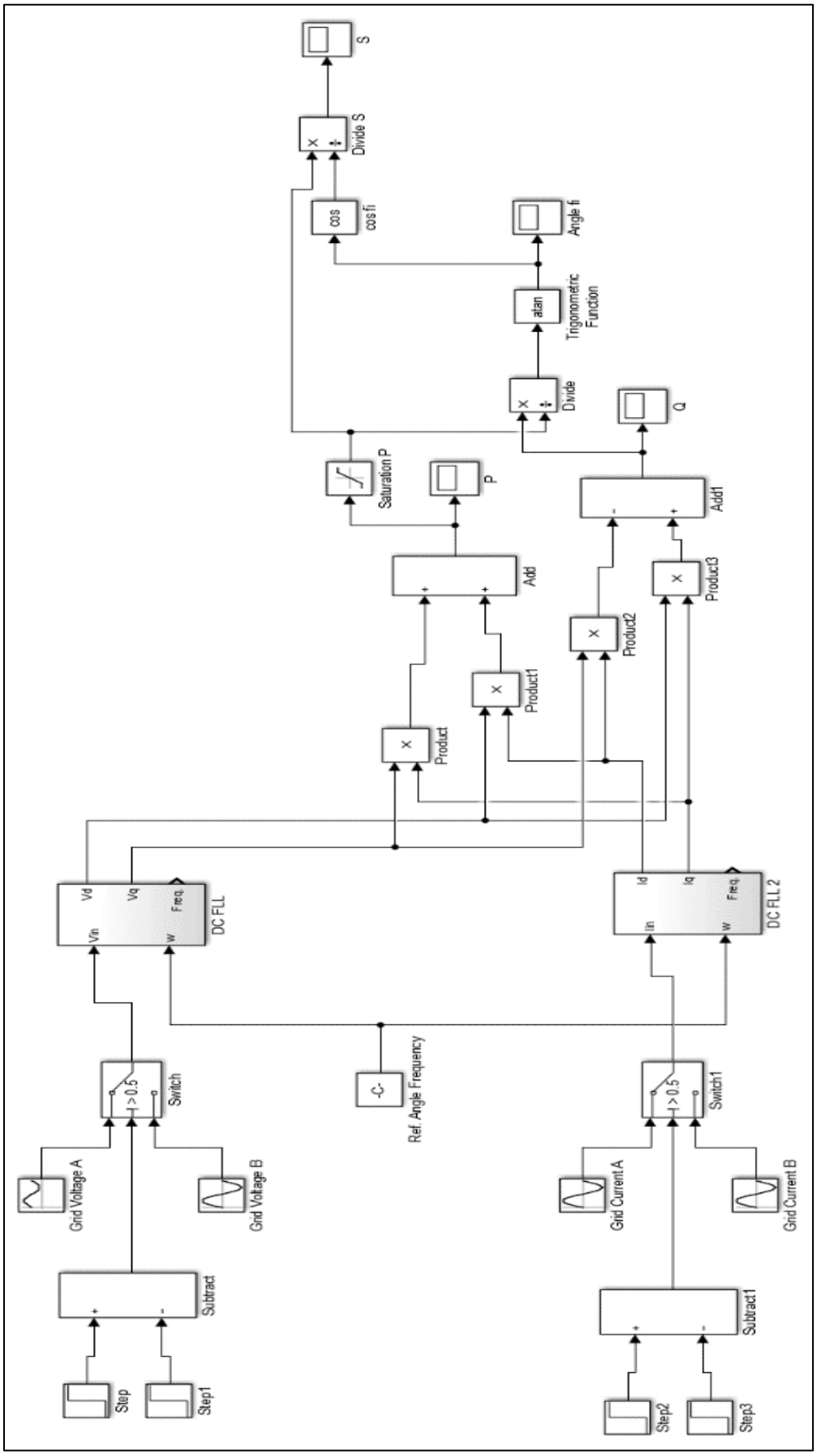
S
Divide S
cos
cos fi
Angle fi
atan
Trigonometric Function
Divide
Q
Saturation P
P
Add1
Add
Product3
Product2
Product1
Product
Vd
Vq
Freq.
Vin
w
DC FLL
Id
Iq
Freq.
In
w
DC FLL 2
Switch
> 0.5
Ref Angle Frequency
Switch1
> 0.5
Grid Voltage A
Grid Voltage B
Grid Current A
Grid Current B
Subtract
Subtract1
Step
Step1
Step2
Step3

This document contains an analysis of several scenarios, which are presented to showcase the capabilities of the FLL system used in this project. Some scenarios may contain multiple issues whereas others will focus on a single fault. Referent input values, for all scenarios, are:

- V = 220 [V]
- I = 5 [A]
- ω = 2*π*50 [rad/sec]
- V – I phase difference scenarios]

A. Scenario 1 Showcase

This scenario intends to show case how the system behaves when the gain of the FLL loop (Γ) is changed. Value of Γ had been optimally set to 50 in all upcoming scenarios. The system will undergo frequency oscillations, albeit, at different values of gain Γ. Additionally, the system will experience phase adjustment.

Figures 7 and 8 show the power measurement for the system when gain Γ is brought down from 50 to 10. By decreasing the value of Γ, the system achieved a stable output in a period, which can be seen from equation (7). The conclusion from this examination is that the system output behaves more oscillatory, as opposed to the optimum value of Γ = 50.

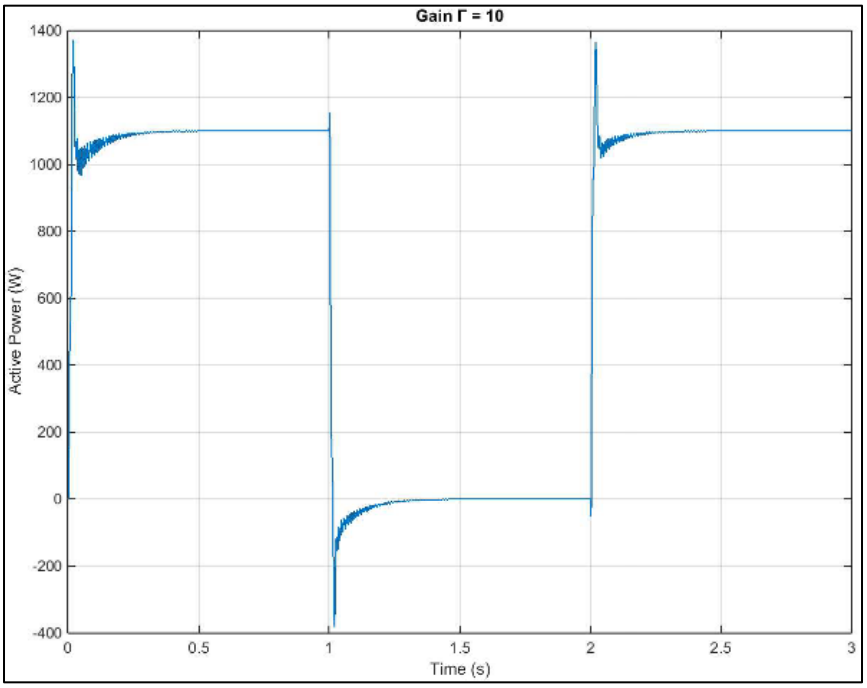

FIGURE 7. Active power for scenario 1 (Γ = 10).

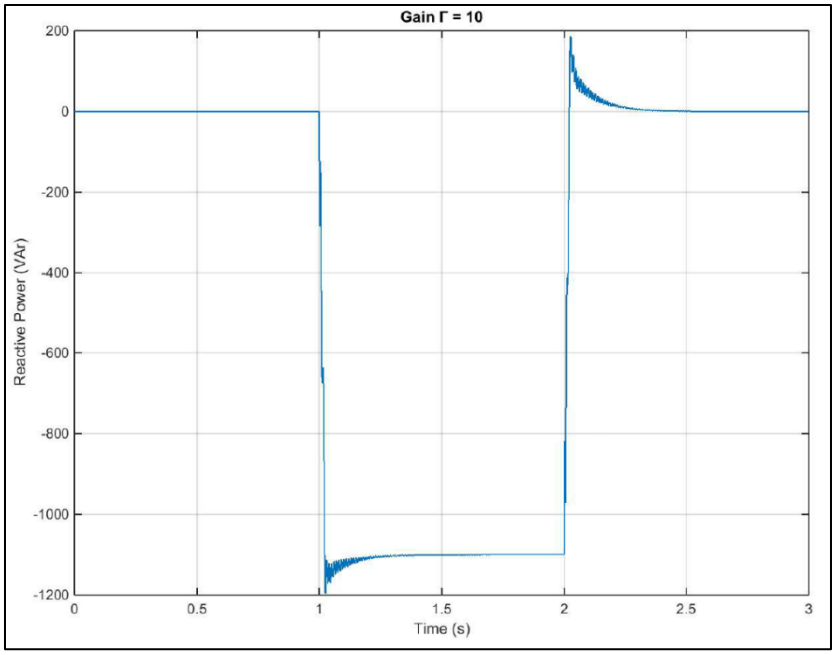

FIGURE 8. Reactive power for scenario 1 ($\Gamma = 10$).

A slower response may not necessarily be a bad thing. Some systems demand lower responses, and in such cases, a lower value of gain Γ may be the optimal solution.

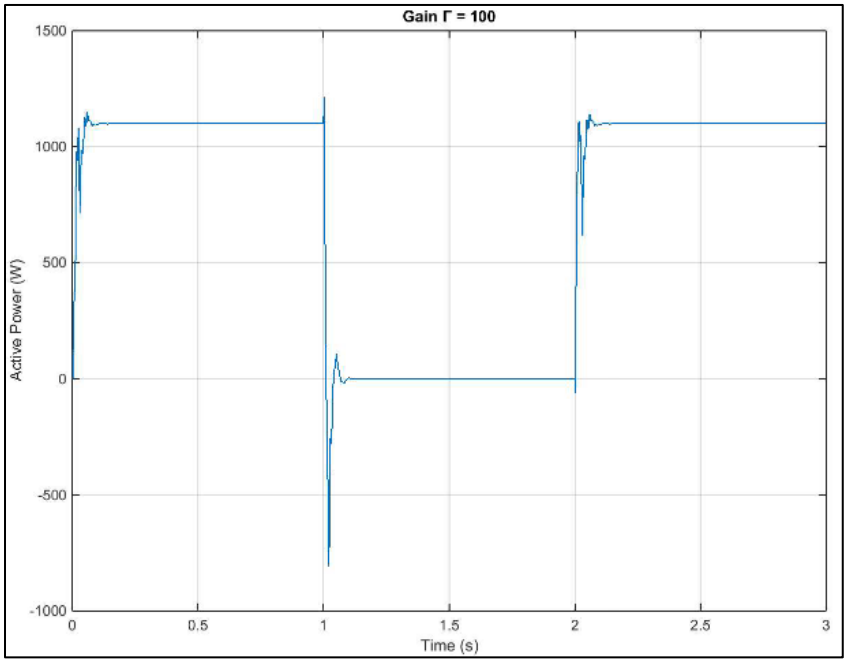

FIGURE 9. Active power for scenario 1 ($\Gamma = 100$).

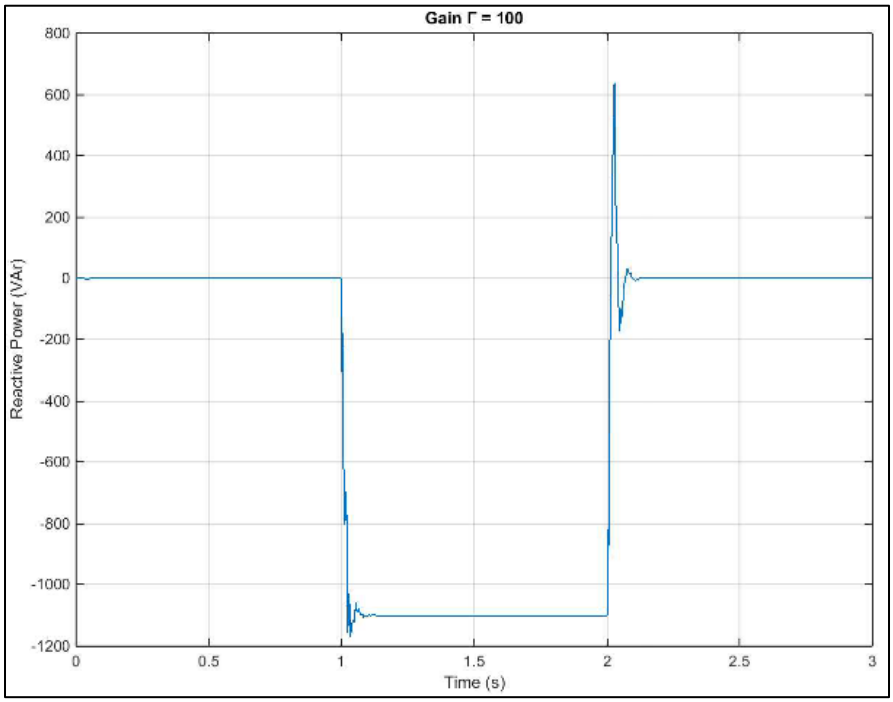

FIGURE 10. Reactive power for scenario 1 ($\Gamma = 100$).

Following the same equation (7), a higher value of gain Γ ought to cause a faster system response. While this may be true in theory, Figures 9 and 10 show the actual stability. The time it takes to stabilise the output is certainly much shorter than in Figure 7. However, the transition process experiences a much greater overshoot, as well as the unpredictable oscillations, before the signal itself is stabilised. This shows that the gain Γ cannot be infinitely increased. The increase depends on the measured system and the need for real-time information. As it was previously mentioned, the optimal value of Γ in this paper was calculated at $\Gamma = 50$.

B. Scenario 2 – Referent Measurement

In scenario 2, the regular operation mode is considered. In this case, there are no faults on the input, as this measurement serves as a reference to all the following scenarios.
Figure 11 shows the graph of active power (*P*). The measured value of *P* is 1100 W. Considering that no changes were present (in comparison to referent values) on inputs, this calculation is a simple multiplication of voltage and current.

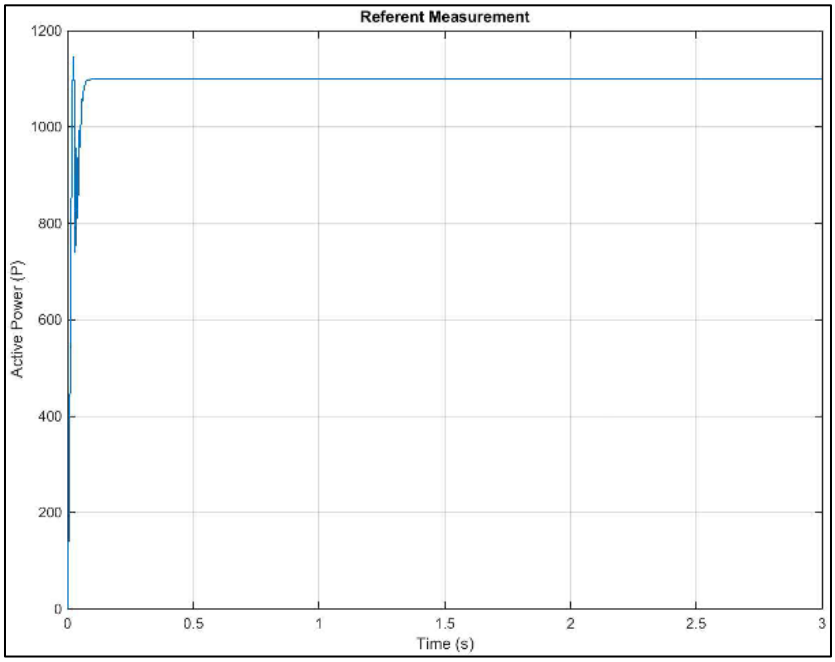

FIGURE 11. Active power for scenario 2.

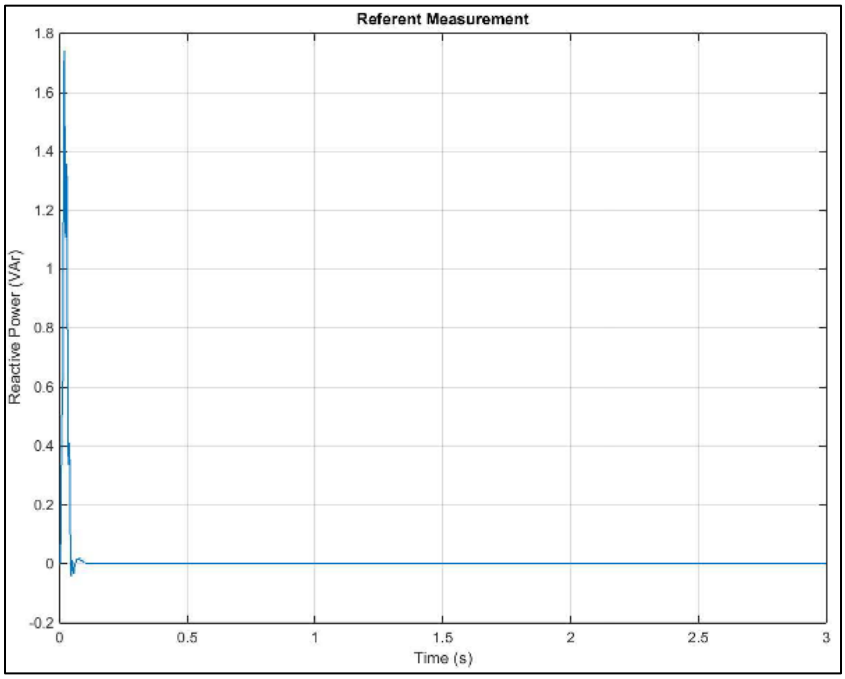

FIGURE 12. Reactive power for scenario 2.

Figure 12 follows the same principle. Since current and voltage are in phase, the value for reactive power (*Q*) is zero.

C. Scenario 3 – Phase Adjustment

Scenario 3 examines the case where the phase of one input (in this case, this is the voltage phase) is shifted during the operation of the system. At t = 1 s, the voltage phase is changed from 0 to $\pi/2$. At t = 2 s, this change is reset, to clarify the system behavior.

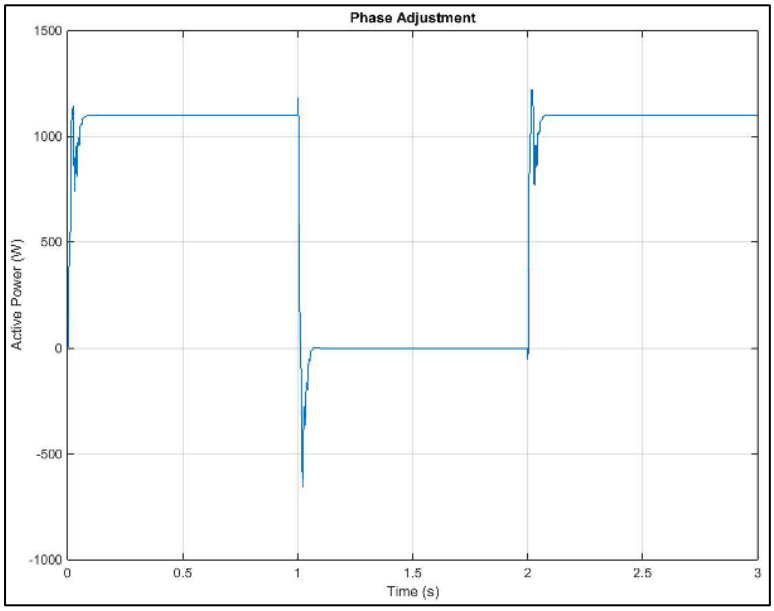

FIGURE 13. Active power for scenario 3.

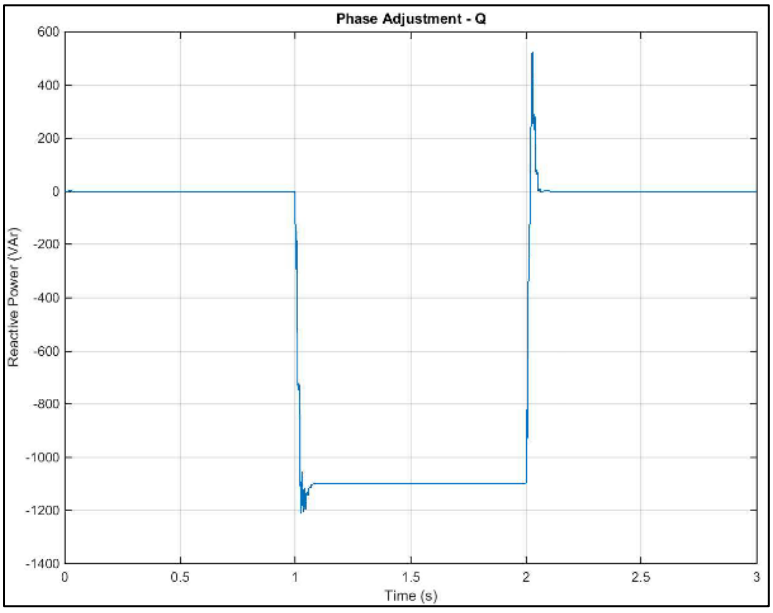

FIGURE 14. Reactive power for scenario 3.

Figure 13 shows active power when the voltage phase is adjusted. For the first second, both

voltage and current are in phase. During this time interval, active power is equal to the referent power in scenario 2, being P = 1100 W. At t = 1 s, the voltage phase switches from 0 to $\pi/2$. During this time interval, until t = 2 s, active power is zero, due to voltage and current having a phase difference of $\pi/2$, leading to ($\cos(\pi/2) = 0$).
Figure 14 shows reactive power for scenario 3. Up until t = 1 s, reactive power is Q = 0 VAr, due to voltage and current being in phase. At t = 1 s, the voltage phase changes to $\pi/2$, leading to reactive power Q = -1100 VAr. Since the voltage phase is the one changing, the angle is $\varphi = -\pi/2$.

$Q = 220\ V * 5\ A * \sin(-\pi/2) = -1100\ VAr$

At t = 2 s and after, the voltage phase goes back to zero, therefore the reactive power goes back to Q = 0 VAr.

D. Scenario 4 – Frequency Oscillation

Frequency values for voltage and current have been known to oscillate in known systems. Due to this fact, the presented FLL system will showcase its behavior when such a change occurs.

For this scenario, a current phase has been set to $\pi/2$. At t = 1 s, both voltage and current go through a step frequency change from 50 Hz to 55 Hz. At t = 2 s, changed values revert to initial ones.

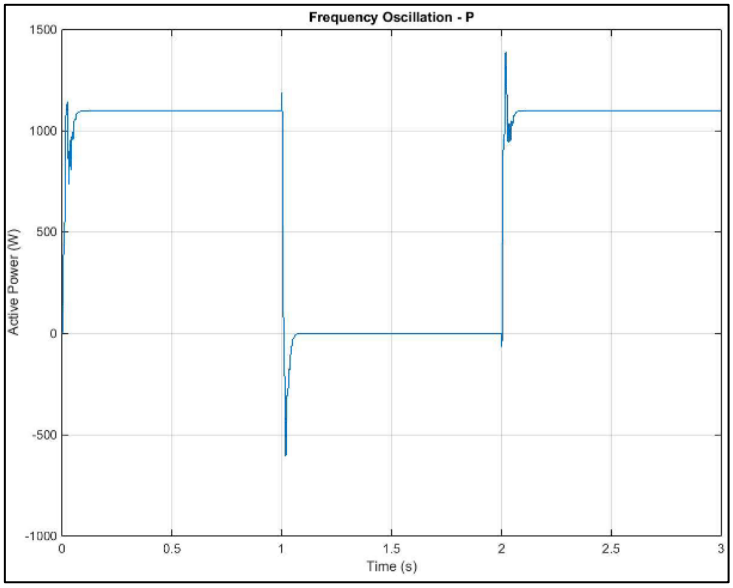

FIGURE 15. Active power for scenario 4.

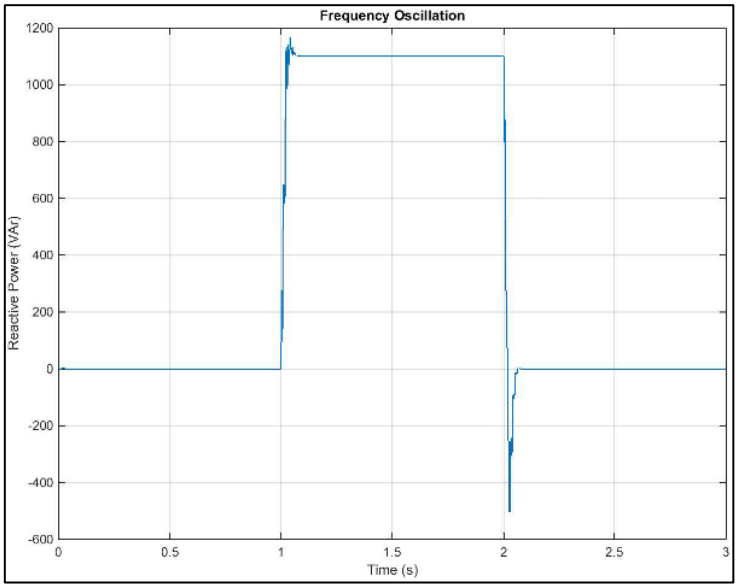

FIGURE 16. Reactive power for scenario 4.

Figure 15 shows the measured active power as frequency oscillations occur. At t = 1 s, frequency values for voltage and current change, and the system clearly shows this through the oscillation of the active power, on the graph. This oscillatory behavior can be affected through the value of Γ. Value of Γ used in this project is deemed to be optimal, however, that can be further debated. Regardless, in a short amount of time, the system recovers, and accurately proceeds to perform the measurement, showing correct values of active power. Similar oscillatory behavior repeats once the measured system restores the initial value of frequency (50 Hz). This measurement is more than satisfactory.
Figure 16 proves that the same logic applies to reactive power, and that the algorithm is capable of solving multiple issues at once.

5. Conclusion

In conclusion, this paper elaborated on the usefulness of the FLL in power measuring systems. While the FLL may be used in different systems, this paper proves the versatility and the capability of the FLL to perform power measuring. The FLL was successfully performed through various problematic scenarios, such as phase adjustment and frequency oscillation.

The power measuring design, shown in the project, greatly reduces the demand for DSP systems, which need to perform integrals and derivatives to calculate powers. Instead, by utilizing the output of the SOGI, simple trigonometry is enough to perform accurate and fast power calculations.

Additionally, the currently present power measuring FLL system can be further improved. It is a menial task to add apparent power and power factor calculations. Another issue that the FLL can resolve is the issue of the DC component which causes major issues in ordinary power measuring systems. However, this topic will be further expanded on in future works. The presented system performed marvelously, completely fulfilling expected results.

6. References

[1] C. f. O. P. o. t. E. Communities, "Towards Smart Power Networks—Lessons Learned From European Research FP5 Projects," 2005.

[2] Blanchard, Phase-Locked Loops - Application to Coherent Reciever Design.

[3] Ciobotaru, M., Teodorescu, R., & Blaabjerg, F. (2006). A New Single-Phase PLL Structure Based on Second Order Generalized Integrator. *37th IEEE Power Electronics Specialists Conference*, 1–6. https://doi.org/10.1109/PESC.2006.1711988

[4] Freijedo, F. D., Doval-Gandoy, J., Lopez, O., & Acha, E. (2009). Tuning of Phase-Locked Loops for Power Converters Under Distorted Utility Conditions. *IEEE Transactions on Industry Applications*, *45*(6), 2039–2047. https://doi.org/10.1109/TIA.2009.2031790

[5] Golestan, S., Guerrero, J. M., Vasquez, Juan. C., Abusorrah, A. M., & Al-Turki, Y. (2018). Modeling, Tuning, and Performance Comparison of Second-Order-Generalized-Integrator-Based FLLs. *IEEE Transactions on Power Electronics*, *33*(12), 10229–10239. https://doi.org/10.1109/TPEL.2018.2808246

[6] Luna, A., Rocabert, J., Candela, J. I., Hermoso, J. R., Teodorescu, R., Blaabjerg, F., & Rodriguez, P. (2015). Grid Voltage Synchronization for Distributed Generation Systems Under Grid Fault Conditions. *IEEE Transactions on Industry Applications*, *51*(4), 3414–3425. https://doi.org/10.1109/TIA.2015.2391436

[7] Rioual, P., Pouliquen, H., & Louis, J.-P. (1996). Regulation of a PWM rectifier in the unbalanced network state using a generalized model. *IEEE Transactions on Power Electronics*, *11*(3), 495–502. https://doi.org/10.1109/63.491644

[8] Robles, E., Ceballos, S., Pou, J., Martín, J. L., Zaragoza, J., & Ibañez, P. (2010). Variable-Frequency Grid-Sequence Detector Based on a Quasi-Ideal Low-Pass Filter Stage and a Phase-Locked Loop. *IEEE Transactions on Power Electronics*, *25*(10), 2552–2563. https://doi.org/10.1109/TPEL.2010.2050492

[9] Rodriguez, P., Luna, A., Candela, I., Mujal, R., Teodorescu, R., & Blaabjerg, F. (2011). Multiresonant Frequency-Locked Loop for Grid Synchronization of Power Converters Under Distorted Grid Conditions. *IEEE Transactions on Industrial Electronics*, *58*(1), 127–138. https://doi.org/10.1109/TIE.2010.2042420

[10] Rodriguez, P., Luna, A., Candela, I., Teodorescu, R., & Blaabjerg, F. (2008). Grid synchronization of power converters using multiple second order generalized integrators. *2008 34th Annual Conference of IEEE Industrial Electronics*, 755–760. https://doi.org/10.1109/IECON.2008.4758048

[11] Wu, F., Sun, D., Zhang, L., & Duan, J. (2015). Influence of Plugging DC Offset Estimation Integrator in Single-Phase EPLL and Alternative Scheme to Eliminate Effect of Input DC Offset and Harmonics. *IEEE Transactions on Industrial Electronics*, *62*(8), 4823–4831. https://doi.org/10.1109/TIE.2015.2405496

[12] Yu, B. (2018). An Improved Frequency Measurement Method from the Digital PLL Structure for Single-Phase Grid-Connected PV Applications. *Electronics*, *7*(8), 150. https://doi.org/10.3390/electronics7080150